Analysis and experiments on C band 200G coherent PON based on Alamouti polarization-insensitive receivers

Research Article | Vol. 30, No. 26 / 19 Dec 2022 / Optics Express 46782
Optics EXPRESS

Analysis and experiments on C band 200G coherent PON based on Alamouti polarization-insensitive receivers

ABIR HRAGHI,[1,*] GIUSEPPE RIZZELLI,[1] ANNACHIARA PAGANO,[2] VALTER FERRERO,[1] AND ROBERTO GAUDINO[1]

[1] *Politecnico di Torino, Department of Electronics and Telecommunications, Torino, Italy*
[2] *TIM, Access Innovatio Department, Torino, Italy*
[*] *abir.hraghi@polito.it*

Abstract: Passive optical network (PON) based on coherent detection has attracted a great deal of attention in recent years as a future solution for 100+ Gbps per wavelength. Particularly for 200G-PON, one of the most attractive options would be to switch to QAM transmission and coherent detection, due to its well know advantages compared to the Direct-Detection approaches used so far in PON. However, coherent technology, extensively used in core networks, has costs that are still perceived as too high for the access ecosystem. In order to perform cost reduction, some groups have studied the option of coherent polarization-independent (PI) detection, since it halves the number of optoelectronic components in the receiver front end. In this paper, we thus present a detailed simulative and experimental investigation of polarization-independent receivers to achieve 200 Gbps transmission in C band using the Alamouti polarization time block coding (PTBC). Our goal is to show what would be the system requirements in terms of optoelectronic bandwidths, laser phase noise and ultimate power budget limitations. We study two different modulation formats: quadrature phase-shift keying (QPSK) and 16 quadrature amplitude modulation (16QAM). We also compare heterodyne and homodyne/intradyne solutions through simulations. As a summarizing result, we experimentally show that 200G PON based on 50 Gbaud-16QAM single-polarization Alamouti coded signals would be possible with today state-of-the-art coherent technologies, demonstrating an Optical Distribution Network loss above 33 dB with 25 km fiber length, a very promising result that is compliant with the PON power budget E1 class.

1. Introduction

Networks operators need to keep pace with the unprecedented growth of bandwidth demand due to new emerging applications (real-time games, Internet of things, etc.) [1]. Access networks are no exception, as they too require an upgrade in data rate, for instance by increasing the capacity of current passive optical networks (PONs). In 2014, the ITU-T G.989.x standardized the next generation PON2 (NG-PON2) which allows transmission of 40 Gbps on four wavelengths, each delivering 10 Gbps [2], [3]. Since then, ITU-T and IEEE committees working on PON standardization have started to work on increasing the data rate per wavelength to higher values [4]. IEEE recently standardized a 25 Gb/s line-rate PON [5], and the International Telecommunication Union-Telecommunication Standardization Sector (ITU-T) has just defined a 50 Gb/s line-rate PON [6]. For future PON generations, the capacity is assumed to be 100 Gbps per wavelength (100G-PON) and beyond [7]. From a physical layer performance point of view, coherent detection seems the natural evolution, particularly for 200 G, given its well-known advantages compared to direct detection [8], [9]. In this scenario, one of the proposed solutions is to try to simplify the hardware complexity by using single-polarization receivers since they would halve the number of components compared to the standard "full-coherent" receiver [10]. The key problem of this

#472470 https://doi.org/10.1364/OE.472470
Journal © 2022 Received 17 Aug 2022; revised 16 Oct 2022; accepted 25 Oct 2022; published 8 Dec 2022

Optics EXPRESS

simplified receiver is to make it insensitive to the received signal state of polarization (SOP) and thus can be realized on single-polarization photonic platforms which, for instance, greatly simplify the design when using silicon photonic technologies. To this end, several design solutions have been proposed for a polarization-insensitive system for PON applications. For instance, PI can be obtained at the receiver (i.e. in downstream at the optical network unit (ONU)) using a simplified coherent receiver based on a polarization beam splitter (PBS). In [11], the PBS is located at one of a 50/50 coupler outputs. In [12], [13] the PBS is included to split the local oscillator (LO) signal. However, the key challenge of this polarization diversity simplified receiver is the monolithic integration of the PBS which increases the cost of the ONU. To avoid this problem, polarization insensitivity can be achieved in a "native" way using transmitter-based approaches, such as Alamouti coding (polarization time block coding) [14], polarization scrambling [15], or differential-group-delay (DGD) pre-distortion [16]. If this kind of PI-operation is implemented in the optical line terminal (OLT), a single polarization heterodyne receiver or phase diversity homodyne receiver can be used at the receiver side without a polarization beam splitter. In a PON, the OLT equipment is shared between all the users and thus obtaining polarization-insensitivity at the transmitter side seems an interesting option to reduce overall cost, making this an attractive solution for downstream direction of a PON link.

Among all the transmitter PI options, various demonstrations have proven that the best performing one is likely the Alamouti PTBC approach. In [17], the experiment of an Alamouti 50 Gbaud-QPSK (100Gbps) coded signal with a simplified heterodyne receiver has been performed. For BER = 4×10^{-3}, a receiver sensitivity of -29.6 dBm at a launch power of 7 dBm was obtained. In addition, the applicability of the phase diversity homodyne receiver based on 3×3 symmetric coupler or on 3-fiber IQ coupler was verified for 100G-PON in [18]. For BER = 3.8×10^{-3} a power budget of 36.4 dB and 33.1 dB was achieved for a receiver with symmetric 3×3 coupler and IQ coupler, respectively. Also, 56 Gbps pulse-amplitude modulation (PAM)-4 PON based on real-valued Alamouti coding and polarization independent homodyne receiver is experimentally demonstrated [19].

In future PON, even higher bit rate may be required and in particular, 200 G would be a candidate solution as a x4 capacity upgrade above the currently standardized 50G-PON [20].

Recently, two lab demonstrations of 200 G PON with 50 Gbaud 16 QAM modulation format and single polarization (SP)-heterodyne detection has been performed [21,22]. In [21], a 29 dB power budget is achieved with 20 km transmission for a BER of 10^{-2}. In [22], a power budget of 32.8 dB (BER = 10^{-2}) is experimentally evaluated using balanced detection (SP-heterodyne receiver) considering 25 km reach. Other solutions for 200 Gbit/s/λ PON system were also demonstrated experimentally, such as the one proposed in [23], based on intensity modulation (4-PAM) and coherent detection.

The motivation of this work is thus to present a detailed analysis of the feasibility of 200 G using the Alamouti approach applied to the PON downstream scenario. Whereas previous works in this area investigated mostly 100G-PON, in this paper we focus on 200 Gbps, analyzing the resulting requirements on the optoelectronic components. We investigated in simulation different options: QPSK and 16-QAM modulations formats, heterodyne and homodyne approaches and different transmitted power. For the most promising solution (16-QAM homodyne), we then confirmed simulation results with off-line processing experiments. As a benchmark, we compare the obtained result with those of a full-coherent receiver.

Our findings show that PI-heterodyne receiver performs better than PI-homodyne receiver in terms of receiver sensitivity due to the insertion loss of the receiver front-end, but requires (at least) twice as much bandwidth for the same bit rate.

The paper is organized as follows. In Section 2, we briefly review the alamouti polarization time block coding (PTBC) concept. In Section 3, we describe the simulation and the experimental setup. The obtained simulation results are then shown in Section 4. In Section 5, we present

Optics EXPRESS

our experimental results and compare it with the simulations of the previous section. Finally, in Section 6, we draw the conclusions.

2. Review on the principles of Alamouti polarization time block coding

In standard dual polarization coherent transmitters, two independent QAM data symbols are generated and sent into two orthogonal states of polarization (X and Y), while in the Alamouti polarization time block coding, the QAM symbols are encoded with a particular structure [24] that enables the use of single-polarization receivers. In PTBC, two consecutive QAM symbols are encoded as shown in Fig. 1(b). In the first time slot t (having the duration of the inverse of the baud rate), the symbols S_1 and S_2 are sent on X and Y polarization, while in the second time slot 2 t, $-S_2^*$ and S_1^* are sent on X and Y (* is the complex conjugate). Therefore, when operated at the same bitrate, the Alamouti approach requires twice the baud rate compared to the conventional dual polarization (DP) transmitter. This is the only important drawback of the Alamouti approach, requiring to double the transmitter optoelectronic bandwidth compared to the DP approach used in long-haul networks.

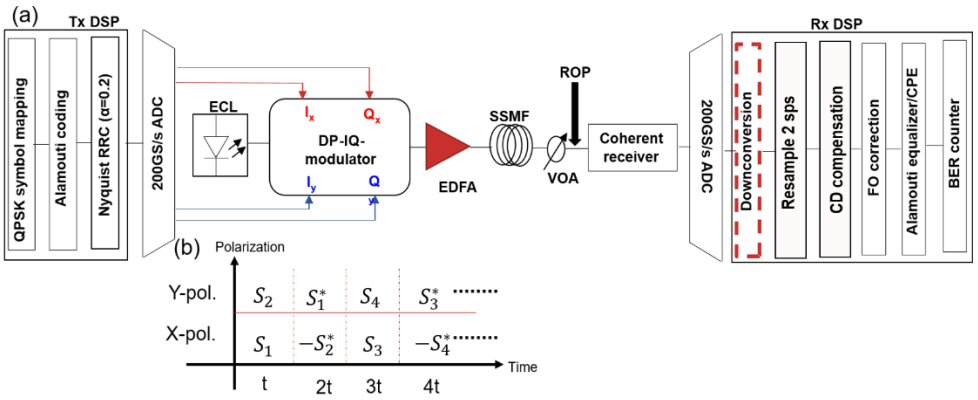

Fig. 1. (a) Simulation and experimental setup. (b) Concept of Alamouti coding [24] (electrical down-conversion block is present only in the heterodyne versions).

Focusing on the polarization evolution, it is well-known that after fiber propagation, the optical field is rotated by the fiber birefringence described by a unitary Jones matrix as follows:

$$\vec{E}_{out} = \begin{bmatrix} h_{xx} & h_{xy} \\ h_{yx} & h_{yy} \end{bmatrix} \begin{bmatrix} E_{in}^{x} \\ E_{in}^{y} \end{bmatrix} \tag{1}$$

At the receiver, only one polarization will be detected (let's assume conventionally the X polarization in the receiver SOP frame), and considering two consecutive time frames we get:

$$S_1^{RX} = h_{xx}e^{j\phi}S_1^{TX} + h_{xy}e^{j\phi}S_2^{TX} \tag{2a}$$

$$S_2^{RX} = h_{xy}e^{j\phi}S_1^{*,TX} - h_{xx}e^{j\phi}S_2^{*,TX} \tag{2b}$$

where ϕ is the laser phase noise. By rewriting this result in matrix form, we obtain:

$$\begin{bmatrix} S_1^{RX} \\ S_2^{*,RX} \end{bmatrix} = \begin{bmatrix} h_{xx}e^{j\phi} & h_{xy}e^{j\phi} \\ h_{xy}^{*}e^{-j\phi} & -h_{xx}^{*}e^{-j\phi} \end{bmatrix}^{-1} \begin{bmatrix} S_1^{TX} \\ S_2^{TX} \end{bmatrix} \tag{3}$$

Optics EXPRESS

Inversion of this matrix is always possible thanks to the fact that the matrix is unitary (at least when Polarization Dependent Loss is negligible), and thus the transmitted information can always be recovered (without loss, as we will show later) independently on fiber birefringence.

3. Simulation and experimental setup

3.1. Transmitter and receiver DSP

The general schematic used for both simulations and experiments is shown in Fig. 1(a). In the transmitter digital signal processing (DSP), we consider either QPSK or 16QAM (using as a source a 2^{15}-1 PRBS), which are then PTBC-coded and then shaped with a square-root raised cosine (RRC) filter with 0.2 roll-off factor. After fiber transmission, we consider different types of coherent receivers. In the receiver DSP, as presented in Fig. 1(a), an analogue-to-digital converter (ADC) digitizes the detected signal. In case of heterodyne detection, in order to evaluate the In-phase (I) and Quadrature (Q) baseband components, an electrical down-conversion is required. Then, the signal is resampled to 2 samples per symbol (SPS) and the chromatic dispersion compensation is applied if needed. In addition, the residual Frequency Offset (FO) is compensated. The usual DSP based on 2×2 MIMO equalization followed by carrier phase estimation (CPE) algorithms used in conventional full-coherent systems cannot be applied to the Alamouti PTBC system due to the phase noise contribution since, as shown in Eq. (3), the conjugation of the even symbols of the received signal causes the conjugation of the phase noise. Therefore, specific equalization and CPE algorithm are required. The Alamouti equalizer is described in [14]. At the input of the equalizer, the received signal is separated into even and odd symbols. Then, the even symbol tributary is conjugated.

The FIR filters are organized in a butterfly structure to allow polarization de-multiplexing. The FIR filters are updated using the least mean square (LMS) algorithm with an optimal convergence step size. The CPE is performed using one-tap LMS algorithm with an optimal convergence parameter. Finally, after symbol-to-bit mapping, the bit error rate is estimated.

3.2. Simulation setup

We ran an extensive numerical simulation for 200 Gbps QPSK and 16QAM transmission systems in "additive white Gaussian noise (AWGN) channel". As shown in [25], the AWGN model is a good approximation for both optically amplified and unamplified systems, since the relevant noise sources in both cases are additive and Gaussian on the detected signal components. The simulations are performed in back-to-back and over 20 km SSMF link which is the standard fiber length used in PON scenario. Assuming C-band operation, the chromatic dispersion and the attenuation of the SSMF are set to 17 ps/nm/km and 0.2 dB/km, respectively. A variable optical attenuator (VOA) is employed to emulate different values of link loss introduced by the PON splitter. Regarding the optical receiver, we used three configurations: PI-heterodyne, PI-homodyne and a dual-polarization full coherent receiver as a reference.

The heterodyne receiver, shown in Fig. 2(a), is composed of a local oscillator laser (LO) properly detuned compared to the transmitted laser, 2×2 optical coupler and one balanced detection followed by a trans-impedance amplifier (TIA). We assume an insertion loss of the 2×2 optical coupler equal to 4 dB. The signal at the output of the balanced detection is centered around an intermediate frequency (IF). The value of the IF should be greater than half of the symbol rate. To down-convert the electrical signal to the baseband (to re-construct the I- and Q-signals), an electrical down conversion is required, as described in Fig. 2(b), which can be implemented on analogue or digital signal processing.

The PI-homodyne (or intradyne) receiver, shown in Fig. 2(c) is based on a 90° hybrid optical coupler, a LO laser approximately at the same wavelength of the transmitted laser, two balanced detectors, and two TIAs. Here we assume an optical loss for the front-end equal to 8.5 dB.

Optics EXPRESS

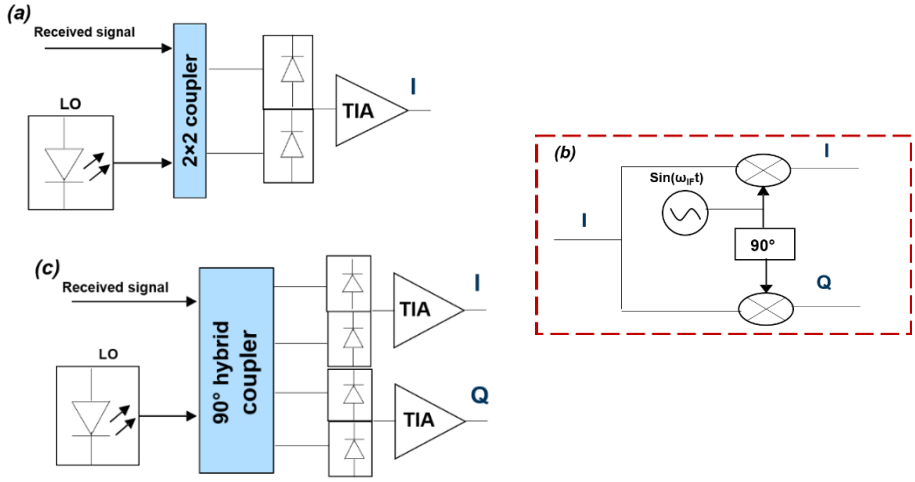

Fig. 2. (a) Polarization independent (PI)-heterodyne receiver, (b) electrical down conversion block. (c) Polarization independent (PI)-homodyne receiver.

This value of the front-end loss is extracted from the intradyne coherent receiver used in our experimental setup. To have a benchmark, we also consider a standard full-coherent receiver, shown in Fig. 3. The total insertion loss in the full coherent receiver, which is due to the 90° hybrid coupler and the PBS, is assumed to be equal to 9.5 dB. Compared to PI-homodyne receiver, the LO power is split in two. In all the receiver configurations, we assume typical values for high bandwidth optoelectronic: the responsivity of the photodiodes is 0.75 A/W, the input-referred noise current density (IRND) of a single trans-impedance amplifier is 20 pA/$\sqrt{}$(Hz) [26] and the laser local oscillator power is fixed to 11 dBm. In our simulation, we have neglected the LO-RIN since we have assumed that the balanced detection is ideal and that the LO has the typical low RIN levels of current laser technology. Using the approach presented in [25], it is possible to estimate that the RIN-induced sensitivity penalty remains negligible (less than 0.3 dB) for RIN values up to -145 dB/Hz provided that the used balance photodiodes have a common mode rejection ratio better than 20 dB.

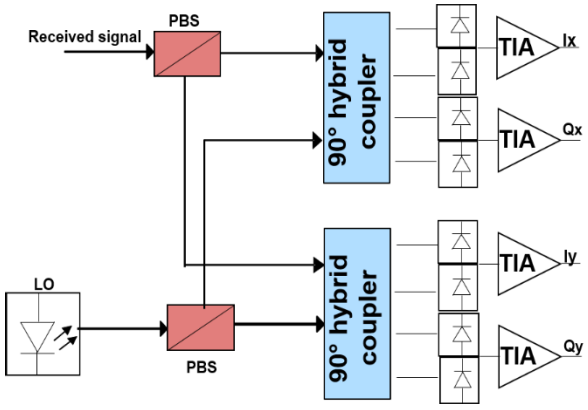

Fig. 3. Polarization and phase diverse coherent receiver (intradyne receiver).

As one of the key parameters, we want to evaluate the performance of the system against the optoelectronic system bandwidth limitation, so that in our simulations we inserted a second

Optics EXPRESS

super Gaussian filter with variable -3dB bandwidth. When relevant, for assessing fiber linear and non-linear propagation effects, we used a standard split-step simulator [27].

3.3. Experimental setup

To validate the simulation results, we also performed experimental measurements on the most promising system to achieve 200 Gbps, i.e. the 50 Gbaud-16QAM with homodyne detection, whose experimental set-up is described in Fig. 1(a). The Alamouti-coded signals are generated offline using the Matlab software described in Section 2. The driving signals are generated using a 92 GSa/s arbitrary waveforms generator (AWG). Then, they are modulated using the LiNbO3-DP-IQ modulator. The transmitter bandwidth is limited by the drivers at the modulator electrical input, which have a 3 dB bandwidth equal to 35 GHz. The optical source is an external cavity laser (ECL) with 100 kHz linewidth operating at 1549.06 nm (and a similar one is used also as a local oscillator at the receiver).

At the output of the DP-IQ-modulator, an erbium-doped fiber amplifier (EDFA) is used to set the transmit power (PTX) to the wanted level, typically around 11 dBm at the input of the optical fiber in most of our experiments. The EDFA is inserted just for practical reasons (availability in our lab), but the target output power could also be obtained using lower-cost semiconductor optical amplifiers (SOA), likely more suitable in the PON ecosystem.

A SSMF of 25 km is used with attenuation and chromatic dispersion equal to 0.2 dB/km and 17 ps/nm/km, respectively. As we have mentioned before the typical target fiber length in PON is 20 km. In our experimental setup, we have used the SSMF available in our lab. The SSMF is followed by a VOA which varies the received optical power in order to measure the receiver sensitivity, as depicted in Fig. 1(a), and emulate the high insertion loss of the PON power splitter. We intentionally did not use optical amplification at the receiver side, having in mind a PON downstream transmission, where the ONU, for cost reduction, should not use optical amplifier. In terms of bit error rate (BER) performance, the receiver is thus limited by the internal "electrical" noise sources inside the coherent receiver (shot noise and TIA thermal noise) which anyway, as discussed in [25], still give rise to an AWGN situation.

In our experimental setup, we used in all cases the front-end of a full coherent receiver (intradyne receiver) as described in Fig. 3, since we want to compare the Alamouti system performance with those of a full-coherent system (used as a benchmark) on the same setup. The receiver is a commercial device (Neophotonics micro-ICR class 40) with a 40 GHz 3 dB bandwidth. The sample rate of the real-time oscilloscope is 200 GS/s, used to acquire 10^6 samples for each measurement. To detect the Alamouti coded signal, we use only the two Ix and Qx signals on one polarization, and we simply discard the other two (Iy and Qy). The total insertion loss of the receiver front-end is 9.5 dB which is due to the 90° hybrid coupler (8.5dB insertion loss) and the PBSs (1dB insertion loss).

4. Simulation results

In this Section, we report simulations results achieved by the setup shown in Fig. 1. In our simulations, the two single-polarization receivers (heterodyne and homodyne) of Fig. 2 and the full coherent receiver of Fig. 3 are compared. In addition, the performance of each receiver is evaluated using two modulation formats (QPSK and 16QAM). Since electrical bandwidth is very critical on high baud rate system, we start by analyzing the achievable optical distribution network (ODN) loss as function of the electrical 3 dB bandwidth of the optoelectronics. The performance is evaluated in back-to-back and over a 20 km transmission distance. To achieve 200 Gbps, the required baud rate for the Alamouti approach is set to 100 Gbaud and 50 Gbaud for QPSK and 16QAM format, respectively. Clearly, the QPSK solution requires an exceedingly high baud rate, but we wanted to keep it in our simulation just in order to have a further reference for discussion. In Fig. 4, we report the resulting maximum ODN loss at $BER_{target} = 10^{-2}$ vs. 3

Optics EXPRESS

dB bandwidth for all cases with optical transmitted power equal to 11 dBm. The heterodyne receiver requires a larger electrical bandwidth compared to the homodyne detection (which is at least doubled for heterodyne receiver) because the signal is modulated in the intermediate frequency (IF). In our case, the IF is equal to 60 GHz and 30 GHz using QPSK and 16QAM format, respectively. To reach 200 Gbps, the required bandwidth, in the case of QPSK format, is equal to 120 GHz and 60 GHz using the PI-heterodyne and PI-homodyne receiver, respectively, which prove that heterodyne detection requires at least double electrical bandwidth compared to homodyne detection. It is important to mention that the optoelectronics components operating at 100 Gbaud are not yet commercially available. In the back-to-back scenario, using QPSK and 16QAM modulation format, the achievable ODN loss is 44.4 dB and 40.8 dB, respectively, with PI-heterodyne receiver. By using PI-homodyne detection, a penalty of 2.4 dB can be observed for both modulation formats. This penalty is due to the loss in the front-end of the receivers since we use realistic front-end components (4 dB insertion loss of the 2×2 coupler in case of heterodyne detection/8.5 dB insertion loss of the 90° hybrid coupler in case of homodyne detection).

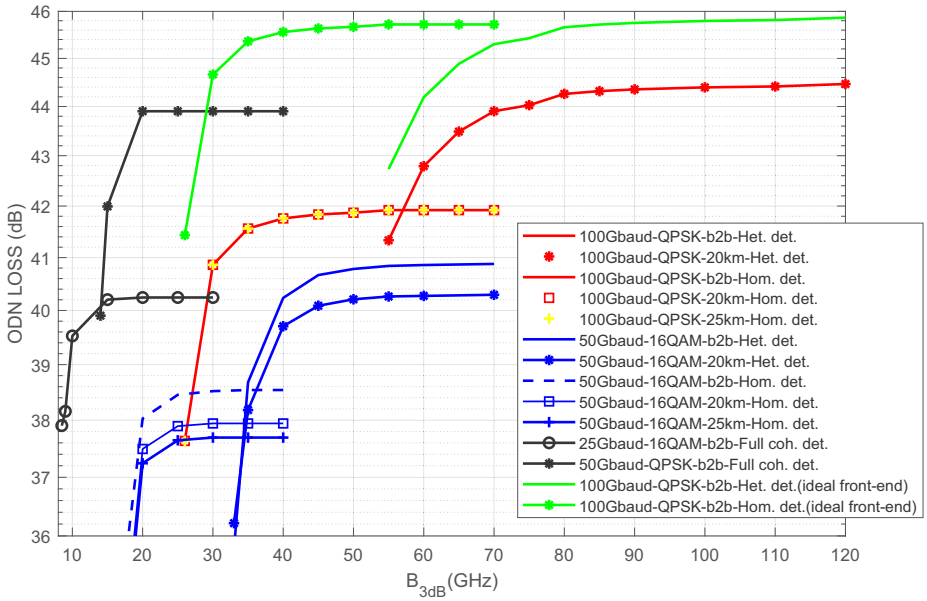

Fig. 4. ODN loss as a function of the electrical bandwidth ($BER_{target} = 10^{-2}$) for QPSK and 16QAM modulation formats using PI-heterodyne, PI-homodyne and full coherent receiver, with P_{TX} equal to 11 dBm.

In our previous considerations, we have inserted realistic insertion loss values for the optical receiver front end. As an ideal comparison, we also present as a benchmark the case of using an ideal front-end on the PI-heterodyne or PI-homodyne receiver (i.e. assuming no extra insertion loss, and in particular 3 dB insertion loss for a 2×2 coupler or 6 dB insertion loss for a 90° optical hybrid, respectively). In this somehow ideal case, it turns out that there is no sensitivity advantage of heterodyne over homodyne for the different QAM techniques [28], but heterodyne receiver requires double electrical bandwidth with respect to the homodyne one. This benchmark situation is shown in the green curves of Fig. 4 for the heterodyne and homodyne QPSK cases. In all other curves, to simulate a realistic system, typical values of the front-end insertion loss used in our simulation are taken from the data sheet.

It is important to mention that in our study, which is focused on the PON scenario, we work in a receiver noise limited case assuming that there is not a receiver optical pre-amplifier but, at

Optics EXPRESS

most, a booster optical amplifier at the transmitter working in a high OSNR situation (we set OSNR = 30 dB in our study, a value that has negligible impact on sensitivity curves).

In Fig. 4 we also show results for 20 km fiber link. Using QPSK format with both PI-receivers, we did not obtain any penalty with respect to the back-to-back configuration. However, for 16QAM, a penalty of 0.6 dB in terms of ODN loss is observed which is due to the onset of fiber nonlinearity for the 11 dBm transmitted power.

As we have mentioned before the 20 km SSMF link is the standard fiber length used in PON scenario. Therefore, we performed the simulation analysis of the preferred 20 km link length. Unfortunately, we could not do so experimentally as the only available SSMF spool in our lab was 25 km long. In Fig. 4, we present the simulation performance of the SP-homodyne receiver using 50Gbaud-16QAM and 100Gbaud-QPSK over 25 km SSMF. For 100 Gbaud-QPSK system, there is no penalty compared to back-to-back or 20 km transmission link. However, in case of 50Gbaud-16QAM, the penalty in terms of ROP increases by 0.25 dB compared to the obtained ROP over 20km SSMF. So, the total ROP penalty for 50Gbaud-16QAM over 25 km SSMF is around 0.9 dB compared to back-to-back configuration.

Focusing on 200G-PON target, the results in Fig. 4 shows that the most promising candidate among all considered options is likely the 50 Gbaud 16-QAM, since the required bandwidth is of the order of 25 GHz, an achievable value with today optoelectronics.

As a benchmark, we also consider in the same figure the full coherent receiver operating again at 200 Gbps, with homodyne detection and thus operating at half baud rate. In this case, by halving the symbol rate for the same bit rate, a 3 dB sensitivity gain should be obtained compared to PI-homodyne receiver (using QPSK or 16QAM). However, according to the results presented in Fig. 4, the full coherent receiver performs better than PI-homodyne receiver only by 2 dB in terms of receiver sensitivity. We can explain this 1 dB penalty by looking at the front-end of the two receivers (Fig. 2(c) and Fig. 3). In the front-end of the PI-homodyne receiver, the PBSs needed to split the received signals and the laser LO signal in full coherent receivers front-end are no longer required. Therefore, the excess loss due to the PBSs reduces the sensitivity advantage from 3 dB to 2 dB.

We then proceeded by studying the tolerance to the fiber nonlinearity effects in order to understand better the previous obtained results at 20 km. In Fig. 5, the achievable ODN loss at $BER_{target} = 10^{-2}$ is reported as function of the transmitted power, after a simulation over 20 km including all linear and nonlinear fiber effects in C-Band. QPSK modulation is much more robust against the fiber nonlinearity compared to 16-QAM, but this second modulation format is more suitable for achieving the 200 G target in particular with the homodyne version (for the aforementioned optoelectronic bandwidth requests) and so we focus our comments on this case. Figure 5 shows that for optimal transmitted power (about +12 dBm) homodyne 16-QAM can achieve more than 38 dB of ODN loss ($BER_{target} = 10^{-2}$). As a consequence, even for the most demanding ODN loss targets (35 dB for ITU-T E2 Class), the graph shows that the system can be designed to work in the "linear region" with transmitter power below 10 dBm. Moreover, comparing this result to back-to-back configuration, a penalty of 0.6 dB (P_{TX} =11 dBm) is observed.

Therefore, the penalty observed in Fig. 4, comparing back-to-back and 20 km transmission in the case of 16QAM, can be explained by the nonlinear impairments showed in Fig. 5.

In Fig. 6, the robustness against dynamic polarization rotations is presented. The polarization is tracked based on the LMS algorithm [29]. Using an optimal convergence step size of the LMS algorithm, the received optical power (at BER_{target}=10^{-2}) is evaluated for different rotation speed (in rad/s) of the received state of polarization (SOP), which is moved on a maximum circle on the Poincaré Sphere). The QPSK is more tolerant to the polarization than 16QAM for both detection techniques, but anyway polarization rotations of up to 1 Mrad/s can be tracked without

Optics EXPRESS

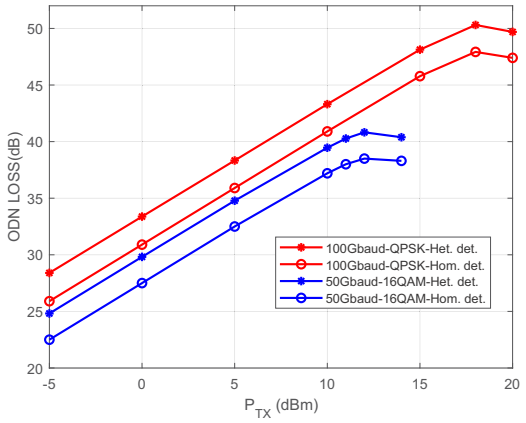

Fig. 5. Achievable ODN loss as a function of the transmitted power for 100 Gbaud-QPSK and 50 Gbaud-16QAM modulation formats ($BER_{target} = 10^{-2}$) with 20 km fiber.

penalty when 16QAM modulation is used, a value that should not give problem in any practical application.

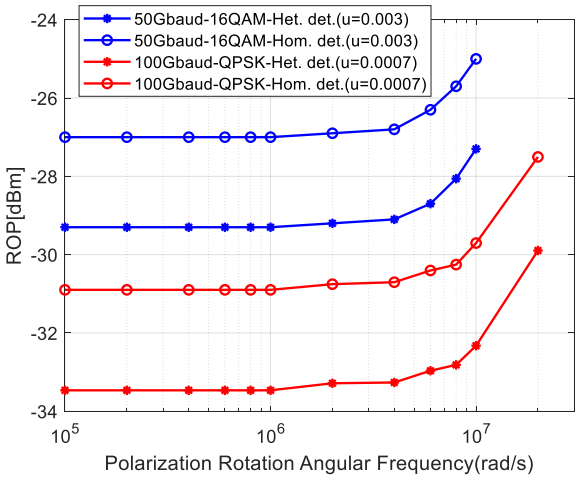

Fig. 6. ROP as a function of the polarization rotation angular frequency for 100 Gbaud-QPSK and 50 Gbaud-16QAM modulation formats ($BER_{target} = 10^{-2}$).

The mitigation of the phase noise is also a crucial issue to be checked for Alamouti systems, which need a particular CPE due to the conjugation of the even symbols of the received signal at the input of the Alamouti equalizer (see the discussion in Sect. 3). In Fig. 7, we evaluate the phase noise tolerance of the 200 Gbps Alamouti coded system using the two PI-receivers under investigation. The received optical power (ROP) obtained for *BER* of 10^{-2}, in back-to-back, is shown as a function of the combined linewidths times symbol duration product ($\Delta\nu T_s$).

The maximum tolerable value of $\Delta\nu T_s$ to have less than 1 dB penalty is 4×10^{-5} (it corresponds to combined 4 MHz laser linewidth at 100 Gbaud QPSK) and 8×10^{-6} (400 kHz laser linewidth at 50 Gbaud-16QAM) using either PI-heterodyne or PI-homodyne receiver. Therefore, distributed feedback (DFB) lasers can be used with QPSK modulation with a linewidth of less than 2 MHz,

Optics EXPRESS

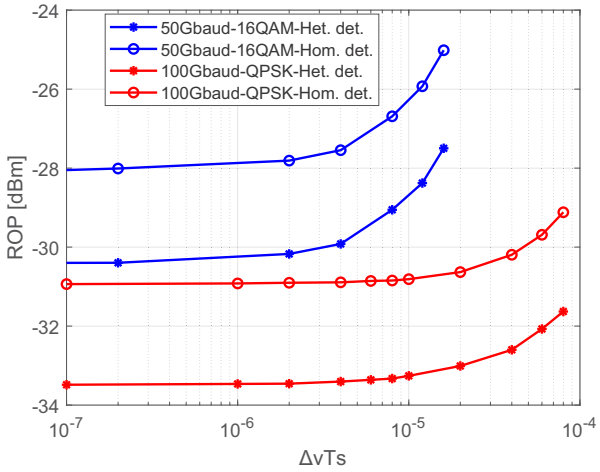

Fig. 7. ROP as a function of combined laser linewidths symbol period product ($\Delta\nu Ts$) for 100 Gbaud-QPSK and 50 Gbaud-16QAM modulation formats ($BER_{target} = 10^{-2}$).

while 16QAM modulation would require narrower linewidth source, like external cavity lasers (ECL).

We also extend our analysis to explore the impact of the transmitter optical amplification on the system performance, which will introduce amplified spontaneous emission (ASE) noise at the receiver side, where the OSNRTX at the output of the transmitter optical amplifier is the metric to quantify this penalty.

In Fig. 8, we thus show the ROP sensitivity at $BER_{target} = 10^{-2}$ vs. the available 3 dB electrical bandwidth for different values of OSNRTX (defined on a bandwidth equal to the baud rate).

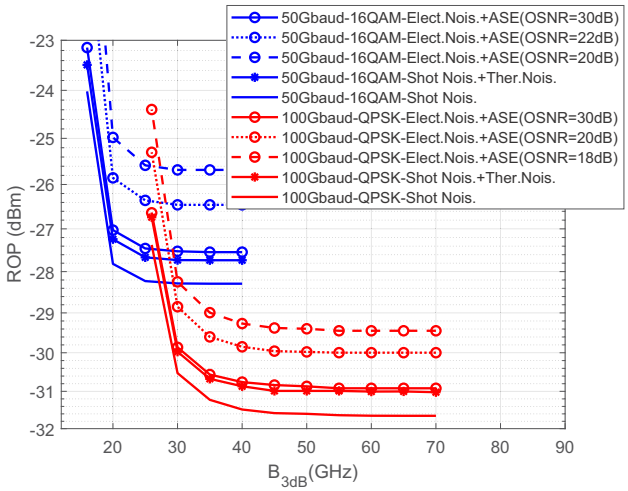

Fig. 8. Impact of the electrical and the optical noise using 100Gbaud-QPSK and 50Gbaud-16QAM modulation format with homodyne detection ($BER_{target} = 10^{-2}$).

The graph shows that as long as the OSNRTX is higher than 30 dB, the additional penalty is negligible (about 0.2 dB can be observed for both modulation formats), while the penalty grows to about 1 dB for OSNRTX = 20 dB for QPSK modulation format, and OSNRTX = 22 dB for 16QAM. Focusing for instance on 50 Gbaud solutions and assuming that a booster SOA

Optics EXPRESS

with Noise Figure F = 8 dB is used after the modulator at the transmitter side, an OSNRTX = 30 dB would require having at least -14dBm optical power at the output of the modulator, which is not a particularly critical constraint. It is important to mention that a small penalty due to preamplifier SOA nonlinearities can be expected for a practical PON implementation. In addition, the performance and scalability of SOA can suffer from the effect of the polarization dependence. The inherent polarization-dependent gain of the SOA, albeit very small in modern devices affects the overall system performance.

In Fig. 8, we also show the impact of the different receiver noise sources (photo detection shot noise and TIA noise). The local oscillator power is equal to 11 dBm, we have used 11 dBm as transmitted power at the input of the optical fiber because the maximum launched power into the ODN is 11 dBm for budget class E2 [30]. A receiver sensitivity penalty equal to 0.7 dB is observed, for both modulation formats, when we add the thermal noise contribution to the shot noise, showing thus that the receiver operates very close to the best possible theoretical conditions (i.e. shot noise limited), an observation that we also verified experimentally. This penalty (0.7 dB) due to the thermal noise is constant for all local oscillator power since the variance of the thermal noise does not depend on the power of the local oscillator. It depends on the input referred noise density (IRND).

Since we are studying a PON scenario with coherent receiver at the ONU side, we are interested also in the impact of the LO power, looking for the LO power level that gives optimal performance. Figure 9 presents the simulation results in terms of BER as a function of the ROP at the input of the PI-homodyne receiver for different values of local oscillator power ranging from 0 dBm to 10 dBm using QPSK and 16QAM modulation formats. As expected, the receiver sensitivity increases by increasing LO power. We observe that performance saturates when the LO power is around 10 dBm, and that a 3 dB ROP penalty is found when the LO power decreases below 2 dBm for both modulation formats. From a system point of view, this kind of analysis can be useful to find the trade-off between best ROP sensitivity performance and LO cost/power consumption.

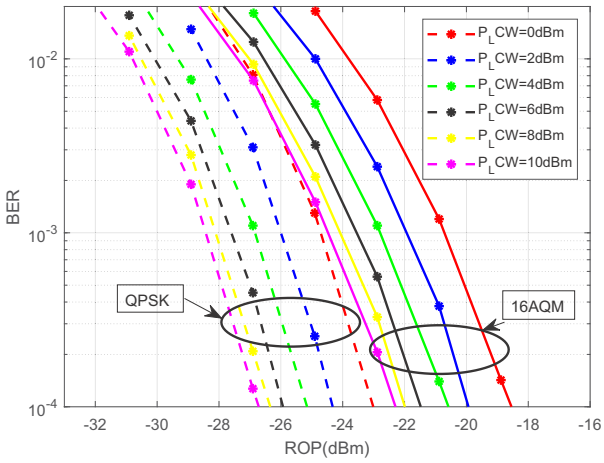

Fig. 9. BER vs. ROP for different local oscillator powers and two modulation formats (QPSK and 16QAM) using PI-homodyne detection.

5. Experimental results

The 200G-PON performances is verified in our study under different conditions in order to analyze in detail the future 200G-PON architectures. First, in our work the performance of the SP-homodyne receiver is compared to the SP-heterodyne receiver in back-to-back (in terms of

Optics EXPRESS

ODN loss) and over SSMF using 100Gbaud-QPSK and 50Gbaud-16QAM modulation formats. QPSK modulation format is used in our study as a benchmark since it gives the best ODN loss.

As a conclusion to this extended simulation study and after analyzing all results, we believe that to achieve 200G-PON using the Alamouti approach, the best option is 16-QAM with homodyne detection, since all other conditions that we studied require a bandwidth for the optoelectronics that appears as too high considering today's technologies.

The 200G-PON performances is verified in our study under different conditions to analyze in detail the future 200G-PON architectures. First, in our work the performance of the SP-homodyne receiver is compared to the SP-heterodyne receiver in back-to-back (in terms of ODN loss) and over SSMF using 100Gbaud-QPSK and 50Gbaud-16QAM modulation formats. QPSK modulation format is used in our study as a benchmark since it gives the best ODN loss.

As a conclusion to this extended simulation study and after analyzing all results, we believe that to achieve 200G-PON using the Alamouti approach, the best option is 16-QAM with homodyne detection, since all other conditions that we studied require a bandwidth for the optoelectronics that appears as too high considering today's technologies. The SP-homodyne receiver is already proposed in [18] based on a 3×3 symmetric coupler and a 3-fiber IQ coupler (for 100G-PON). The contribution of our work is to replace the 3×3 coupler with a 90° optical hybrid and experimentally demonstrate 200G-PON transmission, with a saving in the electrical bandwidth requirements. The experimental results that we show in the following of this Section have two targets: to validate some of the simulation results shown in previous section and, more importantly, to have an actual experimental demonstration of the ultimate limits of the setup.

We will thus show result for 16-QAM at 50 Gbaud, homodyne detection and single-polarization detection, in back-to-back and over 25 km SSMF. In some cases, as a comparison, we will also show results for a standard PM-QAM transmission at the same baud rate and full-coherent detection, that is 400 Gbps transmission. As a benchmark, we show in Fig. 10 the BER vs. ROP curves in this latter case, while in the following Fig. 11 we show the results for the Alamouti system. In these two figures, we varied the LO power, and we performed measurements for back-to-back and for 25 km SSMF (in this case for a transmitted power at the input of the optical fiber equal to 11 dBm). In back-to-back configuration, for a 10 dBm local oscillator power, we have -23.8 dBm sensitivity at BER = 10^{-2} for both the 50 Gbaud DP-16QAM and the 50 Gbaud Alamouti-coded 16QAM signal.

As expected, using the same physical receiver front-end, the DP-16QAM and the Alamouti-coded 16QAM system have the same sensitivity, but with half bitrate in the case of the Alamouti-16QAM system, since a single polarization is detected. Comparing the obtained performance over 25 km SSMF of the two systems to the back-to-back scenario (with a local oscillator power equal to 10 dBm), we observe a penalty of 1.6 dB. This penalty, due to the fiber non-linearity, confirms and validates what was already anticipated by simulations in Fig. 4 and Fig. 5.

We found a different fiber nonlinearity-induced power penalty when comparing the 20 km transmission to the back-to-back scenario (0.6 dB and 1.6 dB respectively in simulation and experiments).

In addition this slight mismatch in penalty values can be due to the mix between linear (chromatic dispersion) and nonlinear (Kerr) effects compensation in the lab experiment (which is hardly as perfect as in the simulation) and in residual jitter in the clocks used in the experiments, which was not taken into account in the simulations.

By decreasing the local oscillator power, the penalty in terms of receiver sensitivity increases. For LO powers of 10 dBm and 2 dBm, a receiver sensitivity (BER = 10^{-2}) equal to -22.3 dBm and -17.6 dBm are obtained, respectively, using the conventional coherent receiver. In case of Alamouti coded system, for the same LO powers (2 dBm and 10 dBm), the full coherent system performs better only by 0.2 dB (-22.1 dBm and -17.4 dBm) in terms of receiver sensitivity. In

Optics EXPRESS

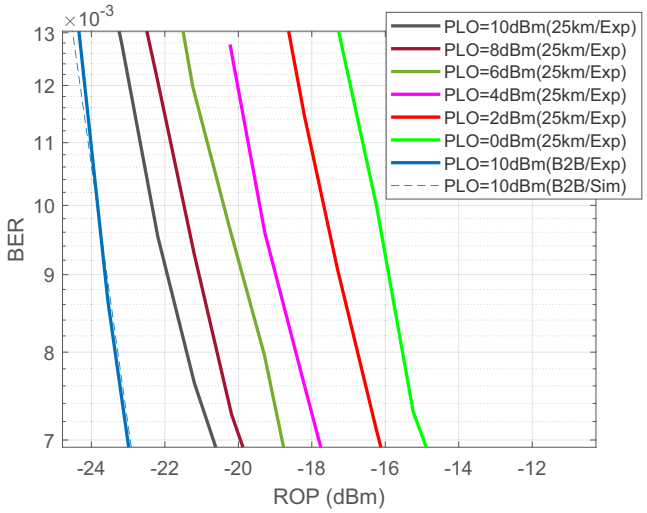

Fig. 10. BER vs. ROP for different local oscillator powers using 50Gbaud-DP-16QAM system with homodyne detection.

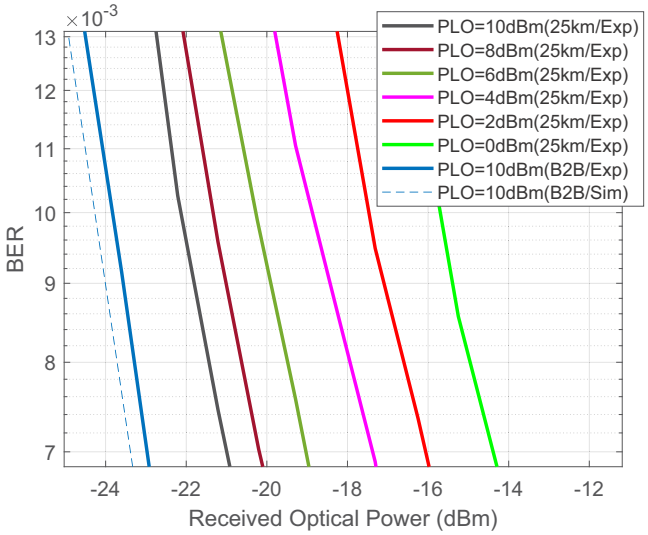

Fig. 11. BER vs. ROP for different local oscillator powers using 50Gbaud-Alamouti-16QAM system with homodyne detection (only one polarization is detected).

back-to-back, we obtain a good agreement between simulation and experimental results, as shown in Fig. 10 and Fig. 11.

The obtained experimental results over 25 km SSMF for different local oscillator powers are compared to the simulation results in terms of receiver sensitivity penalty. Experimental results of both systems, shown in Fig. 12, confirm the simulation results. For a local oscillator power ≥2 dB, the difference between simulation and experimental curves in terms of receiver sensitivity penalty is less than 1dB. This penalty can be due to linear and nonlinear effects compensation in the real experiment which is harder to be perfect as in the simulation, which leads to more power penalty results. Also, simulation and experimental results prove that by using the same receiver front-end, the conventional and Alamouti coded system have the same performance, but with

Optics EXPRESS

half bit rate (operating in the same baud rate) in case of Alamouti system, thus validating the simulation framework presented in the previous Section.

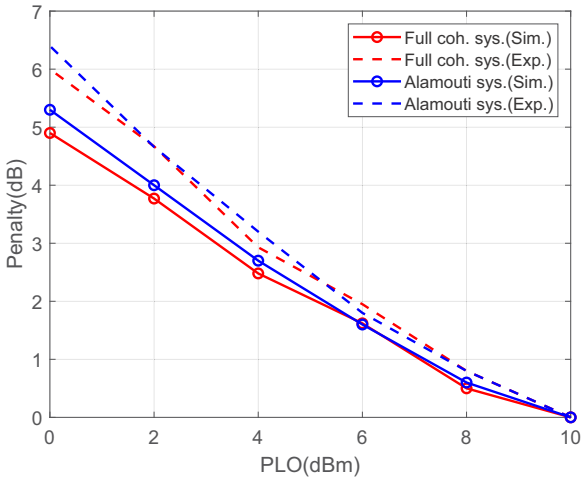

Fig. 12. Penalty in terms of receiver sensitivity as function of the local oscillator power for a $BERtarget = 10^{-2}$ over 25 km SSMF.

6. Conclusion

Focusing on Alamouti 16-QAM with homodyne detection for 200 Gbps coherent PON, we now present some final system indications. Using Fig. 11 and assuming 10 dBm local oscillator power and 25 km SSMF length, we got a ROP sensitivity of -22.2 dBm at $BER_{target} = 10^{-2}$ and 25 km fiber length, using a transmitted power equal to +11 dBm, thus obtaining an optical distribution network loss slightly above 33 dB, a very promising results that would even be compliant with the very demanding PON power budget E1 class (33 dB ODN loss). For this specific system, we have shown in the simulations of Fig. 4 that the required optoelectronic bandwidth needs to be at least 30 GHz, a high but quite reasonable value for today high-end optoelectronics. If and when 200G-PON is commercially deployed (likely in at least a decade from now), the cost of such kind of optoelectronics may have decreased to a level suitable for the access ecosystem.

We finally point out that our experimental results were obtained using a commercial full-coherent front-end (Fig. 3) in which we used only two outputs (i.e. only one polarization branch) since it was the only coherent receiver available in our lab. We point out that this front end, is anyway suboptimal for the Alamouti single-polarization homodyne approach for at least two reasons:

1. A receiver developed ad-hoc for our goals would require a 2×4 optical hybrid (see Fig. 2(c)) and not a 2×8 optical hybrid (see the full-coherent scheme in Fig. 3), and thus the insertion loss on the signal path could be lower. Indeed, in our experiment we detect only a single input signal polarization (we use only one of the two hybrids inside the optical front-end for Alamouti detection), so due to the input PBS, an average loss of approximately 3.5 dB on the average ROP appears with respect to the Homodyne Alamouti receiver of Fig. 2(c).

2. Moreover, the LO laser power does not need to be split on the two polarizations (compare again Fig. 2(c) and Fig. 3), with a consequent decreased insertion loss also in the LO path. Considering the LO power dependence reported in Fig. 9 and Fig. 11, one can consequently also slightly decrease the LO power requirements. Furthermore, in our experiment, the real

Optics EXPRESS

LO power in input to the only one optical hybrid used for Alamouti detection, is reduced by 3.5 dB due to the PBS inside the front-end. It means approximately 6.5 dBm LO power to the hybrid input. Looking at Fig. 12, it means approximately 1.5 dB penalty on the average ROP with respect to the Homodyne Alamouti receiver of Fig. 2(c) where effective LO power was 10 dBm.

We believe this is an important observation, indicating that approximately 5 more dB in ROP sensitivity can be gained compared to the 33 dB ODN loss shown in our final experiments, confirming the potential 38 dB ODN loss as shown in the simulations of Fig. 4. From another point of view, the same considerations shows that there is a system margin for a potential implementation on a single-polarization silicon photonic platform which tends to have higher intrinsic optical losses compared to the high-cost optoelectronic technologies used in the commercial full-coherent, high-end receiver that we used in our experiment.

To conclude, our work presents a complete study of two attractive solutions for future 200G PON. We experimentally verified the use of a SP-homodyne receiver based on a 90° hybrid that requires less electrical bandwidth and lower sampling ratio compared to the SP-heterodyne receiver. This solution facilitates the upgrade of the data rate, particularly for a future 200G-PON environment due to the availability of optoelectronics components with sufficient electrical bandwidth. Anyway, apart from the bandwidth considerations, the SP-heterodyne receiver would be a more cost-effective option than the SP-homodyne receiver, since it requires only one balance photodiode and the 90° hybrid is replaced by a simpler 3-dB coupler with lower insertion loss. Hence, it performs better than SP-homodyne receiver in terms of received optical power (ROP), but with double electrical bandwidth compared to the homodyne receiver. Thus, there is a tradeoff between complexity (half interfaces in case of heterodyne receiver) and required electrical bandwidth (half electrical bandwidth in case of homodyne receiver).

Acknowledgments. This work was carried out inside a research contract with Telecom Italia (TIM). Experiments were performed in the PhotoNext Center at Politecnico di Torino (http://www.photonext.polito.it/).

Disclosures. The authors declare no conflicts of interest.

Data availability. No data were generated or analyzed in the presented research.

References

1. P. Miguelez, "What applications are driving higher capacity in access?" in *2018 IEEE Optical Fiber Communication Conference (OFC,2018)*, 1–3 (2018).
2. "40-gigabit-capable passive optical network (NG-PON2): Series of Recommendation," ITU-TG.989.x, (2014).
3. D. Nesset, "NG-PON2 technology and standards," J. Lightwave Technol. **33**(5), 1136–1143 (2015).
4. V. Houtsma D, V Veen, and E. Harstead, "Recent progress on standardization of next generation 25, 50 and 100 G EPON," J. Lightwave Technol. **35**(6), 1228–1234 (2017).
5. IEEE Std 802.3ca-2020, "IEEE Standard for Ethernet Amendment 9: Physical Layer Specifications and Management Parameters for 25 Gb/s and 50 Gb/s Passive Optical Networks," 2020; https://standards.ieee.org/standard/802_3ca-2020.html, accessed June 2, 2021.
6. Rec ITU-T. G.9804.1, "Higher Speed Passive Optical Networks: Requirements," 2019; https://www.itu.int/rec/T-RECG.9804.1-201911-I/en, accessed June 2, 2021.
7. S. Jia, C. Stengrim, and C. Knittle "Cable Labs Live Webinar: 100 G Single-Wavelength PON Project Launch," Live Webinar, (2021), https://www.cablelabs.com/event/live-webinar-100g-proj-ect-launch.
8. Y. Zhu, L. Yi, B. Yang, X. Huang, J.S. Wey, Z. Ma, and W. Hu, "Comparative study of cost-effective coherent and direct detection schemes for 100 Gb/s/λ PON," J. Opt. Commun. Netw. **12**(9), D36–D47 (2020).
9. A. Shahpari, R. M. Ferreira, R. S. Luis, Z. Vujicic, F. P. Guiomar, J. D. Reis, and A. L. Teixeira, "Coherent access: A review," J. Lightwave Technol. **35**(4), 1050–1058 (2017).
10. M. S. Erkılınç, D. Lavery, K. Shi, B. C. Thomsen, R. I. Killey, S. J. Savory, and P. Bayvel, "Comparison of low complexity coherent receivers for UDWDM-PONs (λ-to-the-User)," J. Lightwave Technol. **36**(16), 3453–3464 (2018).
11. I. N. Cano, A. Lerín, V. Polo, and J. Prat, "Simplified polarization diversity heterodyne receiver for 1.25 Gb/s cost-effective udWDM-PON," in *2014 IEEE Optical Fiber Communication Conference (OFC,2014)*, W4G.2 (2014).
12. E. Ciaramella, "Assessment of a polarization-independent DSP-free coherent receiver for intensity-modulated signals," J. Lightwave Technol. **38**(3), 676–683 (2020).

Optics EXPRESS

13. J. Tabares, V. Polo, and J. Prat, "Polarization-independent heterodyne DPSK receiver based on 3 × 3 coupler for cost-effective udWDM-PON," in *2017 IEEE Optical Fiber Communication Conference (OFC,2017)*, Th1K. 3 (2017).
14. M. S. Faruk, H. Louchet, M. S. Erkılınç, and S. J. Savory, "DSP algorithms for recovering single-carrier Alamouti coded signals for PON applications," Opt. Express **24**(21), 24083–24091 (2016).
15. I. N. Cano, A. Lerín, V. Polo, and J. Prat, "Flexible D(Q)PSK 1.255 Gb/s UDWDM-PON with directly modulated DFBs and centralized polarization scrambling," in *2015 IEEE European Conference on Optical Communication (ECOC, 2015)*, Th.1.3.7 (2015).
16. M. S. Faruk, H. Louchet, and S. J. Savory, "Robust single polarization coherent transceiver using DGD pre-distortion for optical access networks," in *2016 Asia Communications and Photonics Conference (ACP, 2016)*, AF1C.2 (2016).
17. M. S. Erkılınç, R. Emmerich, K. Habel, V. Jungnickel, C. Schmidt-Langhorst, C. Schubert, and R. Freund, "PON transceiver technologies for ≥ 50 Gbits/s per λ: Alamouti coding and heterodyne detection [Invited]," J. Opt. Commun. Netw. **12**(2), A162–A170 (2020).
18. M. S. Faruk, D. J. Ives, and S. J. Savory, "Technology requirements for an Alamouti-coded 100 Gb/s digital coherent receiver using 3 × 3 couplers for passive optical networks," IEEE Photonics J. **10**(1), 1–13 (2018).
19. H. Li, M. Luo, X. Li, X. Zhang, and S. Yu, "Demonstration of Polarization-insensitive Coherent 56Gb/s/λ PAM-4 PON using Real-valued Alamouti Coding Combined with Digital Pilot," in *2019 IEEE European Conference on Optical Communication (ECOC, 2019)*, M.1.F.4 (2019).
20. M. S. Faruk, X. Li, D. Nesset, I. N. Cano, A. Rafel, and S.J. Savory, "Coherent Passive Optical Networks: Why, When, and How," IEEE Commun. Mag. **59**(12), 112–117 (2021).
21. D. Zhang, X. Hu, X. Huang, and K. Zhang, "Experimental Demonstration of 200 Gb/s/λ Coherent PON with a Low-Complexity Receiver and a Multi-purpose Neural Network," in *2022 IEEE Optical Fiber Communication Conference (OFC,2022)*, Th3E.4 (2022).
22. M. S. Faruk, X. Li, and S. J. Savory, "Experimental Demonstration of 100/200-Gb/s/λ PON Downstream Transmission Using Simplified Coherent Receivers," in *2022 IEEE Optical Fiber Communication Conference (OFC,2022)*, Th3E.4 (2022).
23. J. Zhang, J. Yu, X. Li, K. Wang, W. Zhou, J. Xiao, L. Zhao, X. Pan, B. Liu, and X. Xin, "200Gbit/s/λ PDM-PAM-4 PON system based on intensity modulation and coherent detection," J. Opt. Commun. Netw. **12**(1), A1–A8 (2020).
24. M. S. Erkılınç, D. Lavery, K. Shi, B. C. Thomsen, P. Bayvel, R. I. Killey, and S. J. Savory, "Polarization-insensitive single-balanced photodiode coherent receiver for long-reach WDM-PONs," J. Lightwave Technol. **34**(8), 2034–2041 (2016).
25. G. R. Martella, A. Nespola, S. Straullu, F. Forghieri, and R. Gaudino, "Scaling laws for unamplified coherent transmission in next-generation short-reach and access networks," J. Lightwave Technol. **39**(18), 5805–5814 (2021).
26. E. Harstead, R. Bonk, S. Walklin, D. van Veen, V. Houtsma, N. Kaneda, A. Mahadevan, and R. Borkowski, "From 25 Gb/s to 50 Gb/s TDM PON: transceiver architectures, their performance, standardization aspects, and cost modeling," J. Opt. Commun. Netw. **12**(9), D17–D26 (2020).
27. D. Pilori, M. Cantono, A. Carena, and V. Curri, "FFSS: The fast fiber simulator software," in *2017 IEEE International Conference on Transparent Optical Networks (ICTON, 2017)*, We.B1.5 (2017).
28. J. R. Barry and J. M. Kahn, "Carrier synchronization for homodyne and heterodyne detection of optical quadriphase-shift keying," J. Lightwave Technol. **10**(12), 1939–1951 (1992).
29. S. Haykin, *Adaptive Filter Theory*. (Prentic Hall, Englewood Cliffs, NJ, USA, 2001).
30. J.S. Wey, D. Nesset, M. Valvo, K. Grobe, H. Roberts, Y. Luo, and J. Smith, "Physical layer aspects of NG-PON2 standards—Part 1: Optical link design," J. Opt. Commun. Netw. **8**(1), 33–42 (2016).